PRIMARY RESEARCH ARTICLE

Global Change Biology **WILEY**

Interannual variation in rainfall modulates temperature sensitivity of carbon allocation and flux in a tropical montane wet forest

Maokui Lyu[1] | Christian P. Giardina[2] | Creighton M. Litton[3]

[1]Ecology Postdoctoral Research Station, School of Geographical Sciences, Fujian Normal University, Fuzhou, China

[2]Institute of Pacific Islands Forestry, Pacific Southwest Research Station, USDA Forest Service, Hilo, HI, USA

[3]Department of Natural Resources and Environmental Management, University of Hawai'i at Mānoa, Honolulu, HI, USA

Correspondence
Christian P. Giardina, Institute of Pacific Islands Forestry, USDA Forest Service, Hilo, HI 96720, USA.
Email: cgiardina@fs.fed.us

Abstract

Tropical forests exert a disproportionately large influence on terrestrial carbon (C) balance but projecting the effects of climate change on C cycling in tropical forests remains uncertain. Reducing this uncertainty requires improved quantification of the independent and interactive effects of variable and changing temperature and precipitation regimes on C inputs to, cycling within and loss from tropical forests. Here, we quantified aboveground litterfall and soil-surface CO_2 efflux ("soil respiration"; F_S) in nine plots organized across a highly constrained 5.2°C mean annual temperature (MAT) gradient in tropical montane wet forest. We used five consecutive years of these measurements, during which annual rainfall (AR) steadily increased, in order to: (a) estimate total belowground C flux (TBCF); (b) examine how interannual variation in AR alters the apparent temperature dependency (Q_{10}) of above- and belowground C fluxes; and (c) quantify stand-level C allocation responses to MAT and AR. Averaged across all years, F_S, litterfall, and TBCF increased positively and linearly with MAT, which accounted for 49, 47, and 46% of flux rate variation, respectively. Rising AR lowered TBCF and F_S, but increased litterfall, with patterns representing interacting responses to declining light. The Q_{10} of F_S, litterfall, and TBCF all decreased with increasing AR, with peak sensitivity to MAT in the driest year and lowest sensitivity in the wettest. These findings support the conclusion that for this tropical montane wet forest, variations in light, water, and nutrient availability interact to strongly influence productivity (litterfall+TBCF), the sensitivity of above- and belowground C fluxes to rising MAT (Q_{10} of F_S, litterfall, and TBCF), and C allocation patterns (TBCF:[litterfall+TBCF]).

KEYWORDS
annual rainfall, carbon cycling, climate change, Hawaii, mean annual temperature

1 | INTRODUCTION

Long-term soil warming experiments have greatly advanced our understanding of how ecosystem carbon (C) fluxes respond to warming (Hobbie & Chapin, 1998; Liu, Yang, et al., 2017; Luo et al., 2009; Norby & Luo, 2004; Nottingham et al., 2020; Reich et al., 2020; Wood et al., 2019). Results from a large number of primarily temperate experiments and from observational studies across temperate and tropical temperature gradients clearly show that in the absence of moisture limitations to productivity, warming stimulates the flux of C into and the loss of C from ecosystems (Berryman et al., 2016; Bond-Lamberty et al., 2018; Bond-Lamberty & Thomson, 2010; Gherardi & Sala, 2020; Giardina et al., 2014; Litton & Giardina, 2008; Litton et al., 2011; Luyssaert et al., 2007; Melillo et al., 2016; Sistla et al.,

2013). While the impacts of rising temperatures on belowground process rates have received increasing attention (Bradford et al., 2016; Caprez et al., 2012; Fissore et al., 2013; Ziegler et al., 2017), including in tropical systems (Giardina et al., 2014; Nottingham et al., 2020; Wood et al., 2012; Wood et al., 2019), the drivers of these fluxes, in particular the interactive effects of warming and interannual variation in rainfall, remain understudied (Ma et al., 2020; Piao et al., 2020).

Because of the strong link between the canopy and root system of trees (Högberg et al., 2001), net primary productivity (NPP) exerts a strong influence on belowground C processes (Caprez et al., 2012; Litton & Giardina, 2008; Litton et al., 2007). Total belowground C flux (TBCF) is a large component of the forest C budget, accounting for 21–75% of gross primary production (GPP; Litton et al., 2007) and representing the central pathway for delivery of organic C to soils (Giardina et al., 2004). Globally, soil surface CO_2 efflux (F_S) is approximately balanced by TBCF and litterfall (Bonan, 2008; Litton & Giardina, 2008), with variation in TBCF correlating with C decomposition and formation rates (Giardina et al., 2004; Sokol & Bradford, 2019). In a global synthesis spanning diverse forest biomes across a mean annual temperature (MAT) range from −5°C to 28°C, MAT was a strong predictor of GPP, TBCF, and above- and belowground NPP; in contrast, the fraction of GPP partitioned belowground was only weakly related to MAT (Litton & Giardina, 2008). Some evidence indicates that warming-related increases in F_S may exceed those of ecosystem CO_2 uptake (Bond-Lamberty et al., 2018; Ogle, 2018), with important implications for terrestrial C balance. Our research along a highly constrained MAT gradient in tropical montane wet forest showed that MAT-related increases in F_S are best explained by increases in TBCF, litterfall, and litter decomposition rates (Bothwell et al., 2014; Giardina et al., 2014). Paired with increased nutrient cycling rates (Litton et al., 2020), increased C fluxes point to a positive GPP response to MAT. In contrast, we observed no MAT-related variation in ecosystem C storage, soil C storage, or soil C turnover (Giardina et al., 2014; Selmants et al., 2014), highlighting that warming-related constraints on tropical C cycling vary by flux and storage component.

Research directed at understanding whole stand responses to multiple climate change variables is limited. In a meta-analysis of 120 mostly temperate experimental studies manipulating temperature and moisture, NPP decreased with warming while synergistic interactions disappeared at the highest temperatures (Ma et al., 2020). In a grassland study, Reich et al. (2020) found negative effects of reduced moisture on productivity, but positive effects of elevated temperature, moisture, CO_2, and nitrogen. Forest NPP is also strongly regulated by both temperature and precipitation (Drake, Tjoelker, et al., 2019; Litton & Giardina, 2008; Luyssaert et al., 2007; Ma et al., 2020; Sullivan et al., 2020), as well as their interactions (Taylor et al., 2017), but the effects of these interactions belowground are poorly understood (Piao et al., 2020). Interannual climate variation in the tropics affects both temperature and moisture, with implications for the C sink strength of tropical forests (Baccini et al., 2017; Cox et al., 2013). This variation, but also baseline shifts, can transform

an ecosystem from a C sink in cool, wet years to a C source under warmer and drier conditions (Liu, Bowman, et al., 2017; Mitchard, 2018; Taylor et al., 2017). And evidence from a young Eucalypt plantation suggests that artificial warming and drying interact to affect C partitioning and belowground flux (Drake, Furze, et al., 2019; Drake, Tjoelker, et al., 2019). Clearly, variation in precipitation and temperature can drive the timing and magnitude of C process rates (Jung et al., 2011; Poulter et al., 2014).

Climate–C process relationships can be studied via spatial (Raich et al., 1997), temporal (Estiarte et al., 2016), or experimental approaches (Melillo et al., 2002). A spatial approach typically relies on latitude or elevation-driven temperature gradients to understand how variation in MAT affects the compositional, structural, and functional attributes of an ecosystem that regulates above- and belowground C process rates. This approach is sensitive to co-varying, often confounding drivers of process rates, and emphasizes long-term adjustments of a site to mean climate conditions. In contrast, using within-site seasonal or interannual climate variability as a natural experiment (Piao et al., 2020) captures the sensitivity of an ecosystem to short-term temporal variations in weather. Trends can be obscured by lags in the system, however, especially those that operate on scales exceeding weather perturbations (Kannenberg et al., 2020; Sala et al., 2012). Experimental approaches are designed to avoid the confounding influence of co-varying ecosystem drivers by directly altering those climate variables of interest, but this approach also has limitations. Most experimental studies warm only a portion of the ecosystem (e.g., only soils, but see Drake, Furze, et al., 2019; Drake, Tjoelker, et al., 2019), no study has yet to warm the entirety of a mature forest, and experiments are typically short lived (but see Melillo et al., 2016). To address these various limitations, we established a highly constrained 5.2°C mean annual temperature (MAT) gradient in Hawaii to examine how variation in annual rainfall (AR) affects above- and belowground C flux and allocation. This MAT gradient represents a model study system because it is highly constrained (constant vegetation, geology, soil type and age, soil water availability, and disturbance history), simple (low species diversity), and broadly representative (structurally and functionally similar to climatically similar tropical forests), and so is well suited for testing hypotheses about whole forest responses to climate variations (Litton et al., 2020).

Here, we took advantage of a multi-year drought (2008–2011) followed by 3 years of normal then above-normal rainfall (2012–2014) to test the following hypotheses: increasing AR reduces ecosystem C process rates (soil CO_2 efflux, litterfall, TBCF), weakens the response of these fluxes to rising MAT, and shifts C allocation aboveground. Our tests of this hypothesis build on several lines of evidence: (a) increasing AR in tropical montane wet forest is accompanied by increased cloudiness, decreased photosynthetically active radiation, and so reduced GPP; (b) excess supply of substrate is a precondition for enzymatic responses to rising temperature, but a reduction in productivity reduces substrate supply resulting in a weaker MAT response; and (c) increased soil moisture but reduced light shifts constraints on productivity and C allocation from below- to aboveground. To test our hypothesis,

we quantified F_S, aboveground litterfall, and TBCF across our MAT gradient over 5 years during which AR increased from a low of 2843 mm/year in year 1 (2010) to a high of 6403 mm/year in year 5 (2014).

2 | MATERIALS AND METHODS

2.1 | Study site

This study was conducted in nine research plots located between 800 and 1600 m a.s.l., and representing a highly constrained 5.2°C MAT gradient with MAT ranging from 13.0°C to 18.2°C (Litton et al., 2020). All ecosystem measurements were made within the nine 20 × 20 m plots, all of which were located in primary forest on the northeastern slope of Mauna Kea volcano, Island of Hawaii in the Hawai'i Experimental Tropical Forest (HETF; 19°56′41.3″N, 155°15′44.2″W; 600–1800 m a.s.l.), and the Hakalau Forest National Wildlife Refuge (HFNWR; 19°50′31.3″N, 155°17′35.2″W; 600–2000 m a.s.l.). All the plots support mature forests characterized as closed-canopy, *Metrosideros polymorpha*-dominated tropical montane wet forest. Across all plots, 84–97% of stand basal area (BA) excluding tree ferns is comprised of the canopy tree *M. polymorpha* and the midstory tree *Cheirodendron trigynum* (Gaudich.) A. Heller. In addition, an average of 46% of total stand BA consists of three species of tree ferns (*Cibotium* spp.). Overall, plot BA increases while stand density decreases as MAT increases, reflecting large-scale forest level changes (Litton et al., 2011). Coarse woody debris and litter C pools decrease with rising MAT (Iwashita et al., 2013), while litter decomposition rates increase strongly with MAT (Bothwell et al., 2014; Giardina et al., 2014). Across our gradient, above- and belowground live biomass C and soil C storage and turnover do not vary with MAT (Giardina et al., 2014; Selmants et al., 2014). Across our nine plots, soil pH (mean = 3.9), cation exchange capacity (mean = 11.9 cmol/kg), and bulk density (mean = 0.21 g/cm^3) do not vary with MAT; because annual precipitation and evapotranspiration both increase with increasing MAT, soil water balance also does not vary with MAT.

Soils of all plots are all classified as *Acrudoxic Hydrudands* derived from 14 to 65 ky tephra ash deposits from Mauna Kea volcanism (Soil Survey Staff 2010 cited in Litton et al., 2011). Radiocarbon analyses of soils to 1 m indicate that soil substrate in all plots is derived from ~20 ky weathered tephra (Giardina et al., 2014), while underlying Pleistocene-aged Mauna Kea lava flow is dominated by hawaiite and mugearite (Wolfe & Morris, 1996).

2.2 | Environmental measurements

All plots are below the average base height of the trade wind inversion (2225 m; Cao et al., 2007) and within a given year, all receive similar amounts of solar radiation (SR in Table 1; Selmants et al., 2014). Over this 5-year study, rainfall and photosynthetically active radiation (PAR) were measured at three meteorological stations adjacent to plots

TABLE 1 Environmental and stand characteristics of the nine permanent plots along a 5.2°C mean annual temperature gradient in tropical montane wet forests on the Island of Hawaii

MAT (°C)[a]	MAR (mm)[b]	PET (mm/year)[c]	Solar radiation (W m⁻² yr⁻¹)[c]	Stand Density (individuals per ha)[a]	Stand Basal Area (m²/ha)[a]	Live biomass carbon (Mg/ha)[d]		Detrital carbon (Mg/ha)[d]			Total carbon (Mg/ha)[d]
						Aboveground	Belowground	Soil	CWD	Litter	
18.2	4570	2298	201.1	4225	116	97	24.6	194	21.9	2.68	340
17.3	4292	2232	200.9	3300	100	248	59.5	279	21.9	3.82	612
16.7	3975	2214	202.4	3750	97	139	34.2	270	28.8	3.66	476
16.1	3734	2127	204.9	4275	155	417	97.5	254	11.8	4.06	784
16.1	3433	2137	210.1	5875	109	244	58.2	288	33.3	4.28	628
15.5	3181	2211	214.5	3900	102	164	40.5	285	14.4	4.29	508
15.1	3101	2234	216.2	4375	81	177	43.4	250	96.6	3.77	571
13.8	4119	1888	202.6	13,200	54	158	38.9	220	78.1	3.23	498
13.0	3282	1961	213.1	16,400	66	203	49.4	253	66.8	4.98	577

[a]Mean annual temperature (MAT), stand density, and stand basal area from Litton et al. (2011).
[b]Mean annual rainfall (MAR) estimates from the Rainfall Atlas of Hawaii (Giambelluca et al., 2013).
[c]Mean annual potential evapotranspiration (PET) and solar radiation estimates from Giambelluca et al. (2014).
[d]Live biomass carbon, detrital carbon, and total carbon from Selmants et al. (2014); CWD is coarse woody debris.

located at 800, 1116, and 1600 m a.s.l (bottom, middle, and top of the gradient). Observed rainfall data from these stations were used to estimate AR for each plot from the linear relationship between mean AR (MAR) and MAT (r^2 = 0.88, p < 0.001; Litton et al., 2011). Across the three plots, measured AR varied strongly between the wettest and driest years (Figure 1). We estimated total incoming annual PAR for each plot as follows. First, we established a relationship between measured annual PAR and measured annual SR from data collected at the same three meteorological stations (r^2 = 0.76, p < 0.001). We then estimated total incoming annual PAR for each plot using: (a) the above SR to PAR relationship, (b) the measured relationship between SR and MAR (r^2 = 0.91, p < 0.001; Table 1), and (c) estimated AR for each plot. We measured soil temperature (0–10 cm) and volumetric water content (VWC, 0–10 cm) during F_S measurements at eight collar locations in each of the nine plots (Litton et al., 2011).

In this study, we observed mildly seasonal patterns in monthly rainfall amount, with overall higher values in December. For this reason, we lagged calendar year AR by one month to analyze mean annual soil VWC trends (Figure S1). We found a significant positive relationship between one month lagged AR and mean annual soil VWC (r^2 = 0.88, p = 0.001) but not calendar year AR (Figure S1). To understand AR effects on whole ecosystem processes, we aligned all analyses to a 1-month lagged annual AR period.

2.3 | Above- and belowground carbon processes

We measured F_S and litterfall from 2010 to 2014 in each of the nine plots as previously described (Giardina et al., 2014; Litton et al., 2011). Briefly, eight 20 cm diameter PVC collars were installed to a fixed depth in each plot, and F_S measured monthly from January 2010 to December 2013 and quarterly in 2014 with a portable LI-8100 soil CO_2 flux system and a 20-cm survey chamber (LI-COR, Lincoln, NE, USA). We carefully examined and observed no diel influence on F_S across this gradient, and so annual F_S budgets were constructed for each plot from monthly (2010–2013) or quarterly (2014) instantaneous F_S measurements by multiplying mean flux rates by

the number of seconds in the day to scale to g C m^{-2} day^{-1}, averaging daily rates over 12-month period, and multiplying by 365 days. We measured aboveground litterfall monthly from January 2010 to December 2014 by collecting fallen fine litter in eight permanently installed litter traps (0.174 m^2) per plot.

We used mass balance to estimate TBCF as described by Giardina et al. (2014):

$$TBCF = F_S - litterfall + \Delta \left[C_S + C_F + C_R \right]$$

where C_S represents mineral soil C, C_F represents forest floor C, and C_R represents live root C, and TBCF is that photosynthate annually allocated belowground from the canopy to support root production and respiration, root exudates, and symbionts. Estimating TBCF from F_S and litterfall was first proposed by Raich and Nadelhoffer (1989), and improved upon by Giardina and Ryan (2002), who carefully estimated changes in storage in order to precisely calculate by difference how much C must enter the system to account for any losses (F_S) not explained by litterfall or annual changes in C stocks. Based on previous results from our MAT gradient (Giardina et al., 2014) and a nearby study in a rapidly aggrading forest on similar soils (Giardina & Ryan, 2002), we assumed that: (1) soil C was in steady state because there was little variation in soil C or its fractions across MAT and the plots have not seen disturbance for many decades; (2) soil C losses to erosion or leaching are negligible in these closed canopy forests; (3) 10% of TBCF was allocated to coarse root growth; (4) changes in fine root standing stocks are negligible; and (5) the forest floor was in steady state.

Carbon allocation to fine roots represents an important component of TBCF including metabolized exudates, senesced roots, and leached C, which are accounted for as measured F_S in this mass balance-based approach. Regarding assumption (4) then, deviation of the fine root stock from steady state across years would be a concern only if change in fine root storage between years was a significant portion of TBCF. Change in fine root stock is likely a small fraction of TBCF as coarse root standing stock is the great majority of total belowground root biomass and coarse root increment represents ~10% of TBCF.
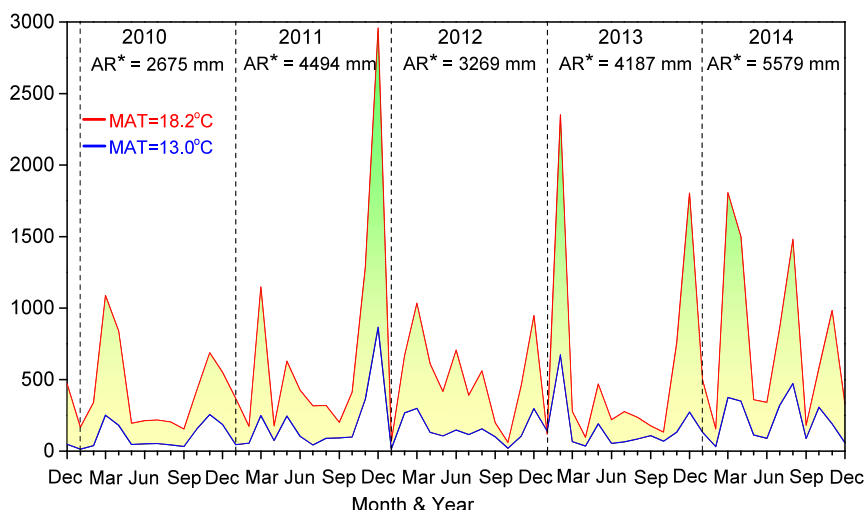

FIGURE 1 Monthly rainfall across the nine MAT plots (from 13.0 to 18.2°C) from 2010 to 2014. Annual rainfall (AR) is the mean of nine MAT plots during each of 5 years. Colors range from yellow to green represent the driest to wettest plots, and all the monthly rainfall of the nine plots are included within this range

We assessed potential errors associated with assumption (5) by constructing a simple monthly litterfall cohort model that integrated observed litterfall rates, forest floor mass, and litter decomposition rates (all measured in our plots) with the goal of simulating realistic steady-state forest floor conditions. Briefly, monthly litterfall cohorts were divided into three fractions: fast, making up 45% of total litter input with a 5-month turnover time; intermediate, making up 30% with a 12-month turnover time; and slow, making up 25% with 24-month turnover time. These turnover times were derived from observed mean decomposition rates in the second half of 2012, an intermediate rainfall year (Bothwell et al., 2014); percentages were adjusting until modeled steady-state forest floor (350 g/m² achieved after 38 months of simulated monthly litter additions) matched mean forest floor mass measured across our gradient (Selmants et al., 2014). We then ran the model for another 3 years using decomposition data from Schuur (2001), which conveniently encompassed an AR range that closely matched our AR range. Specifically, we modified turnover times in a hypothetical dry year 4 (4, 10, and 20 months for the fractions, respectively) and in a hypothetical wet year 6 (14, 34, and 67 months, respectively). This analysis showed that between 2010 and 2013, errors associated with our assumption of steady state would represent an error equaling ~2% of TBCF. In the wet year 5 (2014), modeled forest floor mass increased by 43%, which translates to a 9% underestimate of TBCF. While not insignificant, the magnitude of this error would not change any of the conclusions presented here. Because the second half of year 5 was relatively dry and the decline in decomposition rates in Schuur (2001) stabilized after 4000 mm, the size of this modeled error is likely less than 9%.

2.4 | Data analyses

We used linear regression analyses to determine whether F_S, litterfall, or TBCF varied as a function of MAT within and across years, and 95% confidence intervals (CIs) to describe variation in annual F_S, litterfall, and TBCF across MAT to assess MAT effect sizes. We then used nonlinear regression to determine the influence of AR on MAT effect sizes across 5 years. We used slope values of the relationship between MAT and F_S, litterfall, or TBCF to identify flux increases per 1°C rise in MAT and to calculate apparent temperature sensitivity (Q_{10}). We used nonlinear regression to assess AR and PAR effects on Q_{10} values for F_S, litterfall, and TBCF, and meta-regression to test responses of F_S, litterfall, and TBCF to interannual variation in AR. Statistical analyses were performed in SPSS (SPSS v21, SPSS Inc., Chicago, IL, USA) at α = 0.05.

3 | RESULTS

3.1 | Environmental factors

Total annual rainfall (AR) averaged across the nine MAT plots ranged from a low of 2843 mm in 2010 to a high of 6403 mm in 2014 (Figure 1). Soil VWC was somewhat variable across years, ranging from a mean across plots of 42% in dry year 1 to 55% in wet year 5 (Figure S2). Across plots and years, measured soil temperature was highly correlated with MAT, with the slope of this relationship generally being close to 1 for each of the 5 years (slope range of 0.89–0.99; Figure S3); measured soil temperatures varied by 0.1–0.4°C compared with adiabatic-based estimates of MAT for each plot. Variation in soil VWC across MAT was small, and there were no significant single or 5-year relationships between soil VWC and MAT (Figure S3). Photosynthetically active radiation (PAR) was negatively related to AR ($r = -0.66$, $p < 0.001$) and to daily relative air humidity across all plots ($r = -0.42$, $p < 0.001$; Figure S4).

### 3.2 | Soil respiration, litterfall, and total belowground carbon flux

Averaged across 5 years, F_S, litterfall, and TBCF increased positively and linearly with MAT, with MAT accounting for 49, 47, and 46% of their variation, respectively (Figure 2). Across plots, MAT effects on F_S, litterfall, and TBCF were stronger in the two driest years (AR of 2843 and 3287 mm), with MAT effects in wetter years (AR of 3655–6403 mm) being weak or nonsignificant (Figure 2 and Figure S5). Across years and plots, litterfall C fluxes showed a positive parabolic relationship with AR, while TBCF and F_S declined with AR (Figure 2). The slopes and 95% confidence intervals of the relationships between MAT and F_S, litterfall, or TBCF showed a decreasing trend with increasing AR (Figure 3 and Figure S6). Seasonal patterns in monthly fluxes were apparent at all MATs during each of the 5 years, with both F_S and TBCF generally peaking during summer months with higher PAR while litterfall showed no consistent pattern (Figure S7). Across plots and years, increased AR had negative effects on TBCF and F_S, especially when AR exceeded ~3000–4000 mm/year (Figure 4). PAR and AR were negatively related, and the apparent Q_{10} of F_S, litterfall, and TBCF all decreased with rising AR while increasing with increasing PAR (Figure 5).

Across years and plots, monthly F_S increased linearly with soil temperature, while there were no significant relationships between F_S and soil VWC (Figure S8). At the plot level, increasing precipitation had a slightly negative effect on F_S at cool sites, while having a strong negative effect at warm sites (Figure 6). Overall, the highest F_S values were from warm sites in drier years, with the lowest F_S from cool sites in wetter years (Figure 6).

4 | DISCUSSION

Whole stand studies in the tropics that examine the response of C process rates to temporal climate fluctuations (Toszogyova & Storch, 2019), including the interactive effects of temperature and water availability (Ma et al., 2020; Rillig et al., 2019; Walker et al., 2020), are rare. To address these knowledge gaps, we used a highly constrained model study system to test the hypothesis that AR modulates the response of ecosystem C fluxes and above- and

FIGURE 2 The effect of annual rainfall (AR) and mean annual temperature (MAT) on the aboveground litterfall, total belowground carbon flux (TBCF), and soil surface CO_2 efflux (F_S). The relationship between AR and nine plots averaged aboveground litterfall (a), TBCF (b), and F_S (c) over 5 years where annual rainfall varied from 2843 to 6403 mm. The relationship between MAT and 5-year averaged aboveground litterfall (d), TBCF (e), and F_S (f). Values are means with standard deviations ($n = 9$ or $n = 5$)
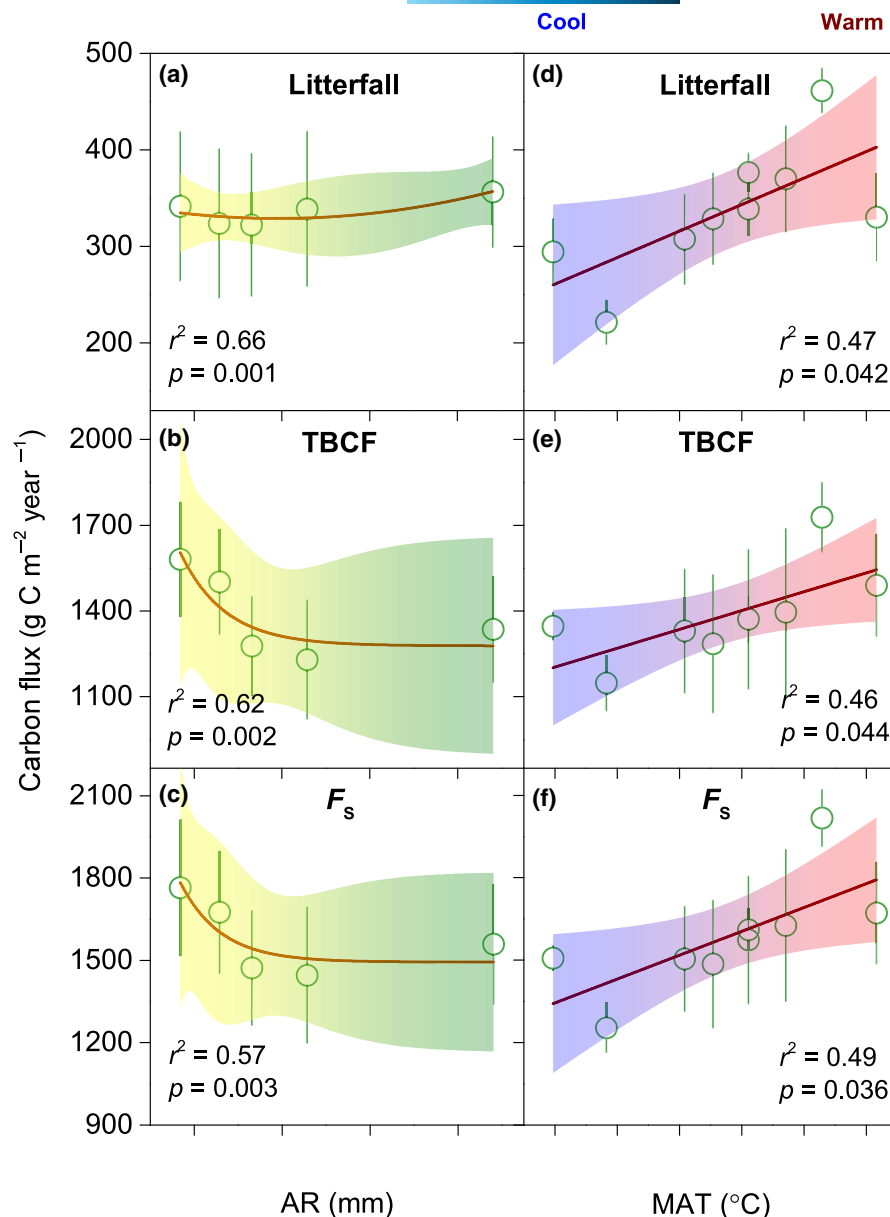
belowground allocation to increasing MAT. We postulated that substrate supply is a biochemical precondition for enzymatic responses to warming (Fissore et al., 2013; Giardina & Ryan, 2000), and that higher PAR from reduced cloudiness in drier years would increase GPP (Nemani et al., 2003) and so belowground substrate supply. In line with allocation theory (Litton et al., 2007), we expected that litterfall and TBCF would increase under drier conditions as would their sensitivity to rising MAT.

In support of our hypothesis, we found that interannual variation in AR strongly affected TBCF, the major source of C to soil (Giardina et al., 2004), and F_S, the major avenue of C loss from soil, as well as their sensitivities to MAT. Conversely, we saw flat or mildly increasing litterfall rates with increasing AR, which conflicts with our hypothesis. One explanation for this discrepancy relates to leaf life span. For the dominant canopy tree (*M. polymorpha*) that makes up most of the litter collected in our plots, leaf life spans of 1–2 years (Cordell et al., 2001) result in lags between foliage production,

senescence, and litterfall. Because litterfall rates were flat or mildly increasing over 5 years of study, leaf life span-driven litterfall lags cannot explain the lack of a negative AR effect on litterfall across the 5-year study period.

An alternative explanation for flat or mildly increasing litterfall rates with rising AR involves the fraction of canopy mass that senesces each year, and senescence rate interactions with leaf life span and foliage production rates. One set of interactions could include light-driven declines in leaf life span *plus* constant foliage production rates. A second includes light-driven declines in leaf life span that exceeds the declines in foliage production rates. A preceding high light year could modify these interactions by increasing foliage production rates but lowering senescence rates in the previous year. We did not collect canopy leaf area data to estimate canopy mass, nor did we track leaf birth and death rates to estimate leaf life span across years. However, given what is known about light effects on leaf life span and senescence (Brouwer et al., 2012), and
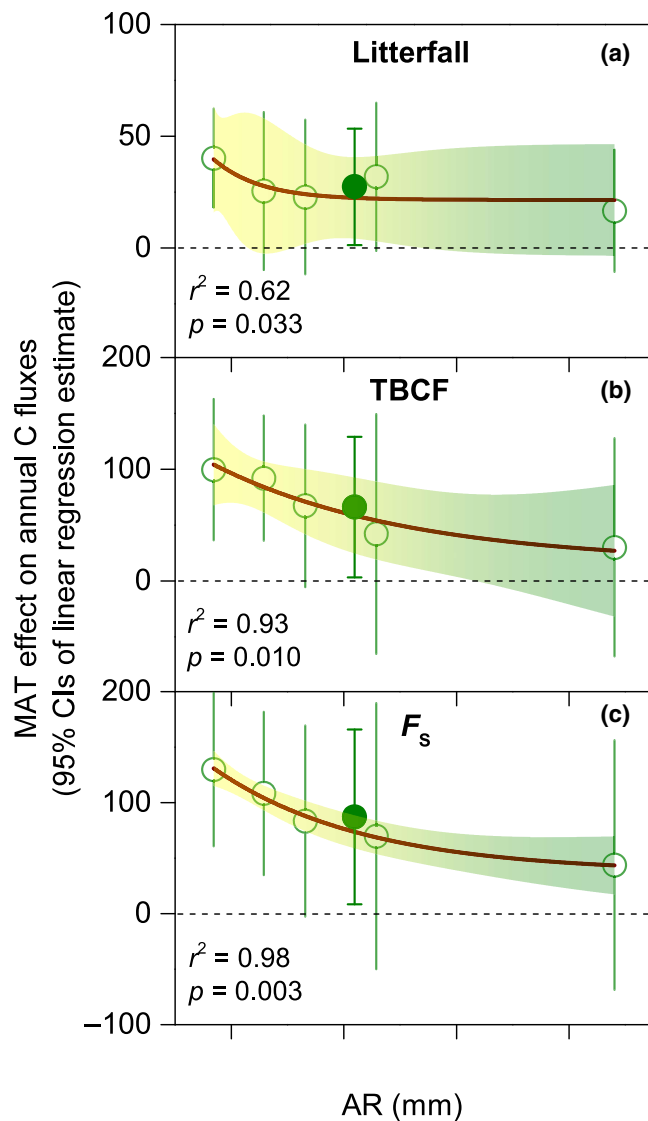
FIGURE 3 The effect of variation in interannual rainfall on the relationship between mean annual temperature (MAT) and aboveground litterfall, total belowground carbon flux (TBCF) and soil surface CO_2 efflux (F_S). The trends of 95% confidence intervals (CIs) of aboveground litterfall (a), TBCF (b), and F_S (c) caused by MAT over 5 years where annual rainfall varied from 2843 to 6403 mm, and the 5-year average; the 95% CIs of linear regression estimates represents the effect size of MAT on the litterfall, TBCF, and F_S, values are means with lower and upper bound of 95% CIs. Open and filled symbols are the 95% CIs of the relationship between MAT and litterfall, TBCF, and F_S for individual years and 5-year average, respectively. The errors bars do not cover "zero" (dash line) represent significant relationships between MAT and litterfall, TBCF, and F_S ($p < 0.05$)

environmental controls on allocation (Litton et al., 2007), the above explanations represent plausible adjustments to a multi-year trend of increasing AR and so light availability. Both interactions require small, whole plant allocation adjustments to reduced light levels and reduced GPP, with the former representing an adaptation strategy and the latter a mass balance constrained short-term response.

The decline in TBCF relative to litterfall likely reflects allocation responses to shifting resource constraints on GPP. Higher soil moisture and moisture-driven increases in nutrient supply in wet years would reduce belowground constraints on productivity (Li et al., 2020), perhaps more so for warm sites where nutrient availability is higher (Litton et al., 2020; Pierre et al., 2017). In contrast, associated increases in cloudiness would enhance light limitations on productivity. Summing litterfall and TBCF, an integrated index of stand level productivity, we observed declines in wet versus dry years with stronger declines in higher MAT plots (Figure 6). Comparing TBCF:[litterfall+TBCF] across MAT and years shows the largest ratios occurring under cool dry conditions (intermediate productivity, low VWC and nutrients, high light); intermediate ratios under cool wet (low productivity, VWC, nutrients, and light) or warm dry (high productivity, low VWC but high nutrients and light) conditions; and the lowest ratio under warm wet conditions (intermediate productivity, high VWC and nutrients, low light). These findings indicate that stand level responses to AR and MAT are dynamic, operate independently, and reflect complex constraints on GPP.

Our finding that the response of belowground C process rates to MAT is more pronounced under conditions of low AR and high PAR aligns with recent findings for individual young, planted Eucalypt trees showing that short-term warming can increase GPP and reduce partitioning belowground (Drake, Furze, et al., 2019; Drake, Tjoelker, et al., 2019). The responses we observed to interannual variation in moisture across our MAT gradient conflicts, however, with their finding that summer rainfall reductions reduced GPP but did not affect partitioning. Our results also conflict with a recent meta-analysis of global change experiments showing that reductions in moisture reduce NPP, and that these moisture-related NPP reductions offset warming-related increases in GPP (Song et al., 2019). The difference between our study and these previous findings may relate to the wet nature of tropical montane wet forests. Alternatively, differences may relate to the fact that experimental temperature and moisture manipulations are decoupled from atmospheric changes (e.g., cloudiness) that often accompany changes in AR.

Finally, in support of our substrate supply hypothesis, we found that variation in the sensitivity of C flux rates to rising MAT was strongly related to AR (Figure 6). Specifically, the proportion of the variation in F_S explained by MAT ranged from 74% in the driest year, to just 11% in the wettest year (Figure S5), primarily as a consequence of AR-related changes in the response of litterfall and TBCF to rising MAT (Figures 3 and 4). As with litterfall (Litton et al., 2007), TBCF is strongly correlated with productivity across MAT (Litton & Giardina, 2008), and so increased sensitivity of F_S to warmer temperatures is most easily interpreted as resulting from the positive effect of declining AR but increasing PAR on GPP. The modulating influence of AR aligns with anticipated global change impacts on GPP and GPP partitioning (Hartmann et al., 2020; Litton & Giardina, 2008).

Forest GPP typically varies positively with MAT (Litton & Giardina, 2008; Luyssaert et al., 2007), but in strongly water-limited systems such as grasslands or dry forests, the temperature sensitivity of GPP can be weakened by the effects of increased precipitation
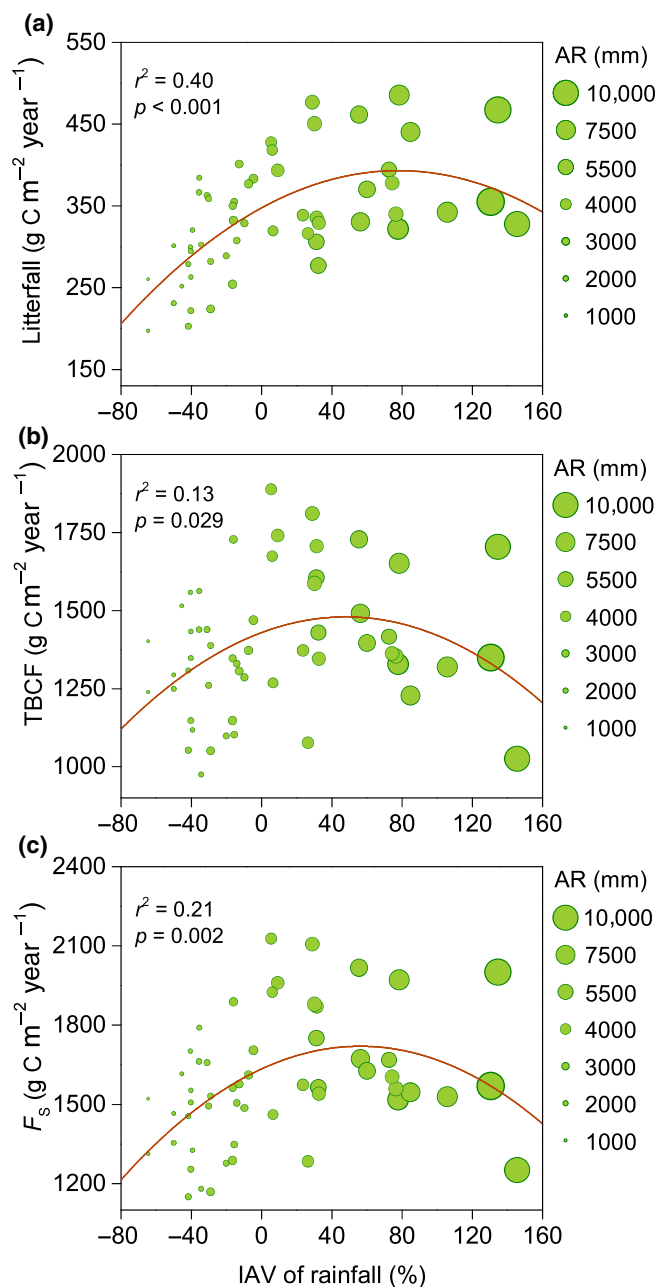
FIGURE 4 Relationship between interannual variability (IAV) of rainfall and aboveground litterfall, total belowground carbon flux (TBCF), and soil surface CO_2 efflux (F_S). Circle size represents annual rainfall (AR) of each plot across five measurement years

and so available soil water on photosynthesis (Knapp et al., 2017; Sullivan et al., 2020). Likewise, Taylor et al. (2017) reported that in tropical forests where MAP is above 3000 mm and MAT is below 20°C, a climate envelope that encompasses our study, increases in AR can negatively affect aboveground NPP. In contrast, Liu et al. (2016) found that in high MAT (~28°C) and low MAP (<2000 mm/ year) forests, positive responses of F_S to changes in precipitation, including the Q_{10} of F_S, were driven primarily by changes in soil moisture. In this meta-analysis of six sites, F_S decreased by up to 18% in response to reduced rainfall while increased rainfall increased

F_S by 11%. This finding is in line with those for drier forests where increases in AR stimulate NPP and TBCF (Taylor et al., 2017) and findings that global variation in NPP is explained by a positive albeit weak ($r^2 = 0.28$) relationship between moisture and plant productivity (Chu et al., 2016). While we cannot determine the cause of our litterfall changes with increasing AR (Figure 2a; see discussion above), AR-related declines in TBCF+Litterfall and their temperature sensitivity (Figure 5) do suggest a negative effect of AR on GPP.

A GPP-driven reduction in TBCF paired with allocation responses to shifting constraints on GPP also reasonably explains the effect of AR on F_S. Reductions in the supply of substrate belowground would drive declines in microbial and root metabolism (Berryman et al., 2016), with such a reduced supply of newly allocated photosynthates belowground explaining the reduced sensitivity of TBCF and F_S to rising MAT (e.g., Fissore et al., 2013). Finally, in our study of tropical montane wet forest, there were significant negative relationships between soil moisture and F_S for warmer plots but not cooler plots or all plots combined. This pattern could be driven by higher nutrient availability in warm plots (Litton et al., 2020; Pierre et al., 2017), with nutrient supply influencing how interannual variation in AR modulates MAT effects on the magnitude and temperature sensitivity of above- and belowground C fluxes.

The observed inverse relationship between rainfall and F_S has other potential explanations: (a) suppressed microbial decomposition due to precipitation-related changes in soil moisture (Liptzin & Silver, 2015; Schuur, 2001); (b) rainfall-induced changes to soil moisture that might also cool soils and so reduce temperature-driven plant transpiration (Maes & Steppe, 2012); (c) changes in soil microbiomes; and/or (d) changes to nutrient supply (Li et al., 2020). Evidence in support of these additional explanations is mixed. The first explanation does not align with results from our study of well-drained soils, which show that soil moisture rarely reached levels that result in suppression of microbial processes. In considering the second explanation, nearly all physiological ecology research indicates that variation in soil temperature affects the activity of plants and microbial decomposers (Bradford et al., 2016; Wood et al., 2019). However, interannual variation in temperature was small, as would be the resulting effects of this variation on C processes; within each of the nine plots, measured annual soil temperature across 5 years diverged by 0.1–0.4°C from modeled MAT.

We cannot directly address the third explanation because we did not measure interannual variability in bacterial or fungal community structure or biomass. We do note that despite large changes in C and nutrient fluxes (Giardina et al., 2014; Litton et al., 2020), soil bacterial community composition is relatively stable across our MAT gradient (Selmants et al., 2016). And in line with data from forested sites across a subtropical elevational gradient (Yang et al., 2020), unpublished data from our MAT gradient also reveal little variation in fungal biomass with MAT (unpublished data of D. Leopold). Regarding the fourth alternative explanation, increases in AR above a long-term mean could affect nutrient cycling rates by alleviating water constraints on decomposition rates, or conversely by reducing belowground O_2 supply thereby limiting nutrient availability
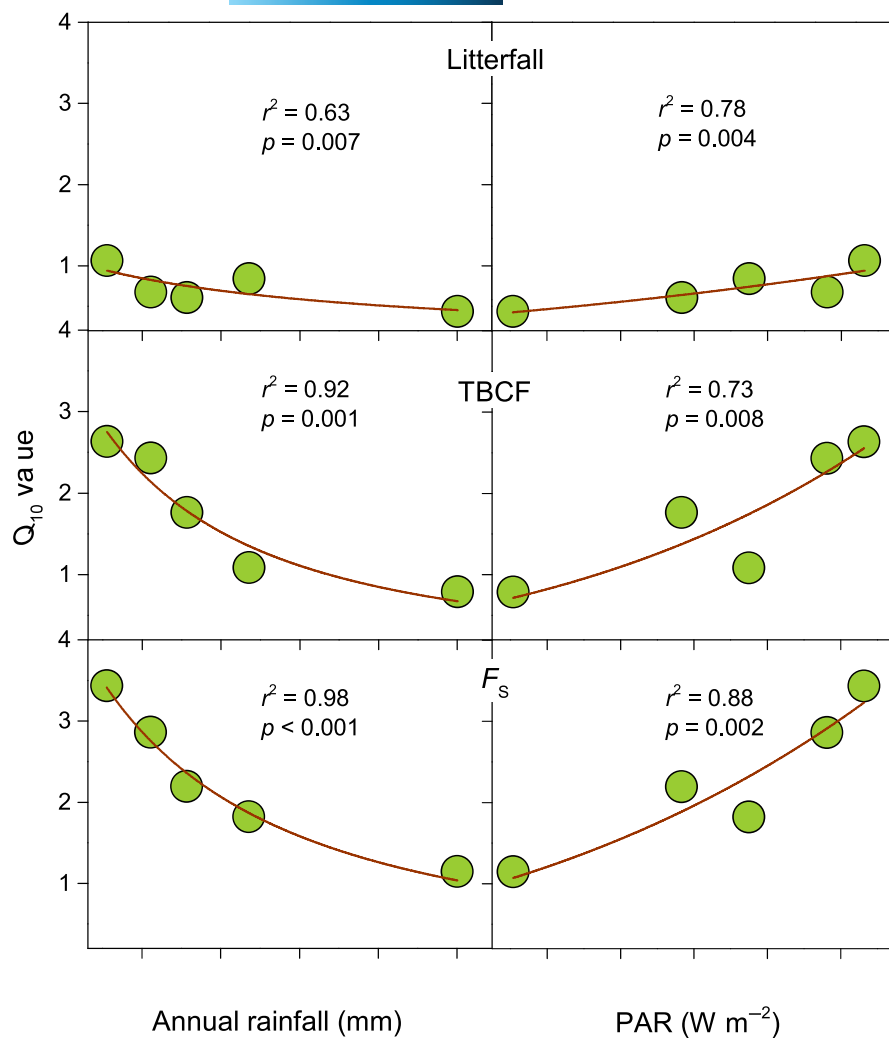
FIGURE 5 The effects of annual rainfall and mean annual photosynthetically active radiation (PAR) on the apparent temperature sensitivity (i.e., Q_{10} values) of aboveground litterfall, total belowground carbon flux (TBCF), and soil surface CO_2 efflux (F_S)
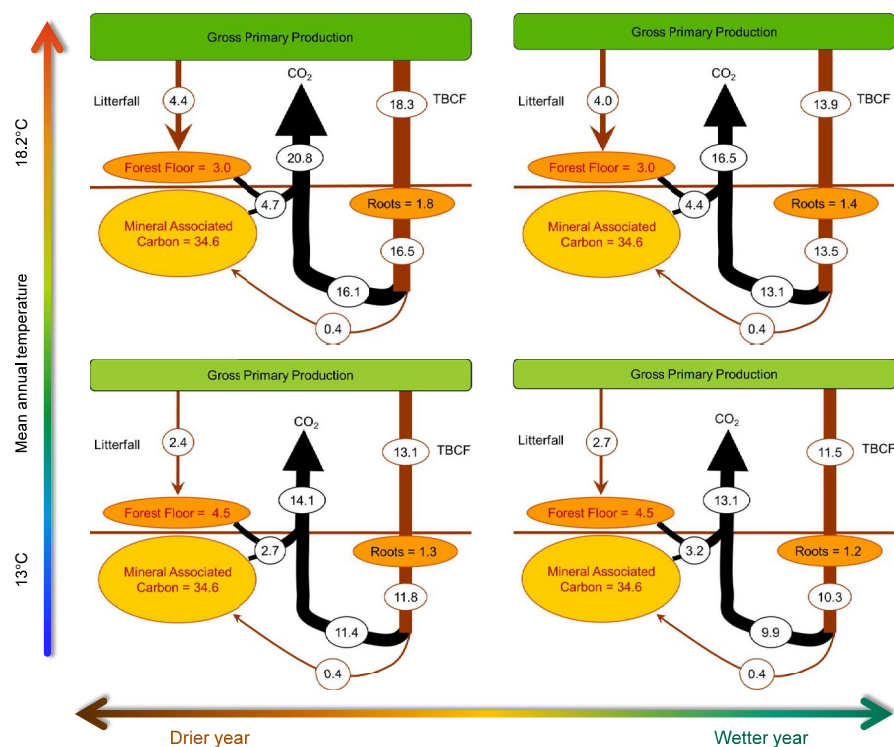

FIGURE 6 Ecosystem response of belowground C processes to interannual variation in rainfall and increasing mean annual temperature. Input fluxes (Mg C ha^{-1} yr^{-1}) are in brown, output fluxes (Mg C ha^{-1} yr^{-1}) are in black, and stocks (Mg C/ha) are in light (soil) or dark (forest floor and roots) orange. Root increment is estimated to be 10% of TBCF. Combining stock and bulk soil organic carbon mean residence time estimates, decomposing SOC is calculated to contribute to <5% of F_S, with a mean contribution to efflux of 0.39 Mg C ha^{-1} yr^{-1}

and uptake for plant growth (Fahey et al., 2016; Rustad et al., 2001; Taylor et al., 2017). Because increases in nutrient availability can strongly increase C supply via enhanced photosynthesis (Binkley & Fisher, 2019), which in turn alters above- and belowground C flux and partitioning (Li et al., 2020; Litton et al., 2007), any factor that reduces nutrient availability could also weaken productivity responses to MAT with impacts to belowground partitioning of GPP (Binkley et al., 2004; Fahey et al., 2016; Giardina et al., 2003; Li et al., 2020; Ma et al., 2020). Overall, the strong positive effect of MAT on nutrient cycling rates and litterfall (Giardina et al., 2014; Litton et al., 2020; Pierre et al., 2017) contrasts the small effects of rising AR on litterfall.

The weak evidence for these four alternative explanations contrasts the strong evidence supporting the more parsimonious interpretation that: (a) AR-related increases in cloud cover drove decreased light availability, which in turn reduced GPP that was expressed across our plots as reduced F_S and TBCF (Figure 6); and (b) decreasing light paired with increasing soil moisture drove an aboveground shift in the partitioning of GPP, expressed across our plots as reduced F_S and TBCF, and slightly increasing litterfall rates. An important contribution of this study then is demonstrating that interannual variability in ecosystem C flux rates can be linked to climate-driven changes in canopy photosynthetic capacity (Litton et al., 2007; Musavi et al., 2017; Piao et al., 2020; Richardson et al., 2007).

Solar radiation is the strongest climatic factor driving forest productivity in tropical ecosystems (Fyllas et al., 2017; Jung et al., 2017), and so any factor that affects light availability (e.g., cloudiness) will impact photosynthesis. The magnitude of these effects can be quite large. Nemani et al. (2003) reported that in rain forests of the Amazon, drought reduced cloudiness and the subsequent increase in solar radiation led to strong increases in NPP. Similarly, Oliphant et al. (2011) showed that minor droughts in tropical forests increase light availability and canopy photosynthesis, while increased precipitation decreases photosynthesis. Furthermore, interannual changes in light availability can drive variation in leaf area of tropical rain forests (Myneni et al., 2007), which can explain up to 82% of the interannual variations in modeled NPP (Wang et al., 2017). Finally, high precipitation can also cause leaf stomata to close, reducing gas exchange and so GPP (Girardin et al., 2010; Goldsmith et al., 2013; Skelton et al., 2017).

Our MAT gradient integrates long-term adjustments by plants and soils to rising MAT, including the direct effects of warmer temperatures on canopy processes combined with direct and indirect effects on C and nutrient supply (Giardina et al., 2014; Litton et al., 2020). Because of the compact and highly constrained nature of our MAT gradient, these adjustments are relatively small and occur in the absence of spatial variation in SR (Selmants et al., 2014), variation typically encountered across latitudinal but also many elevational MAT gradients. The long-term ecosystem responses to MAT across our study are distinct from those identified by Walker et al. (2020), who showed that short-term experimental warming responses of 83 different whole ecosystem variables could over-predict long-term responses. In this regard, our results align with those from temperate zone studies in showing important differences between short-term responses (e.g., seasonal variations in temperature) and long-term adjustments to MAT (Caprez et al., 2012). Furthermore, the flux changes observed with increasing AR may not capture long-term adjustments of these ecosystems to baseline AR change. From our results, however, steadily increasing AR over 5 years resulted in reduced TBCF, which permitted sustained foliage production under reduced GPP. These findings highlight how climate change responses can reflect complex interactions among multiple constraints (i.e., temperature, moisture, nutrients, light) on GPP and whole stand allocation.

CONFLICTS OF INTEREST

The authors declare no conflict of interest.

ORCID

Maokui Lyu https://orcid.org/0000-0002-9567-2170
Christian P. Giardina https://orcid.org/0000-0002-3431-5073
Creighton M. Litton https://orcid.org/0000-0001-5521-1188

REFERENCES

Baccini, A., Walker, W., Carvalho, L., Farina, M., Sulla-Menashe, D., & Houghton, R. A. (2017). Tropical forests are a net carbon source based on aboveground measurements of gain and loss. *Science*, *358*(6360), 230–234. https://doi.org/10.1126/science.aam5962

Berryman, E., Ryan, M. G., Bradford, J. B., Hawbaker, T. J., & Birdsey, R. (2016). Total belowground carbon flux in subalpine forests is related to leaf area index, soil nitrogen, and tree height. *Ecosphere*, *7*(8), e01418. https://doi.org/10.1002/ecs2.1418

Binkley, D., & Fisher, R. (2019). *Ecology and management of forest soils* (pp. 347). Wiley.

Binkley, D., Stape, J. L., & Ryan, M. G. (2004). Thinking about efficiency of resource use in forests. *Forest Ecology and Management*, *193*(1), 5–16. https://doi.org/10.1016/j.foreco.2004.01.019

Bonan, G. (2008). Forests and climate change: Forcings, feedbacks, and the climate benefits of forests. *Science*, 320(5882), 1444–1449. https://doi.org/10.1126/science.1155121

Bond-Lamberty, B., Bailey, V. L., Chen, M., Gough, C. M., & Vargas, R. (2018). Globally rising soil heterotrophic respiration over recent decades. *Nature*, 560(7716), 80–83. https://doi.org/10.1038/s41586-018-0358-x

Bond-Lamberty, B., & Thomson, A. (2010). Temperature-associated increases in the global soil respiration record. *Nature*, 464(7288), 579–582. https://doi.org/10.1038/nature08930

Bothwell, L. D., Selmants, P. C., Giardina, C. P., & Litton, C. M. (2014). Leaf litter decomposition rates increase with rising mean annual temperature in Hawaiian tropical montane wet forests. *PeerJ*, 2, e685. https://doi.org/10.7287/peerj.preprints.609v1

Bradford, M. A., Wieder, W. R., Bonan, G. B., Fierer, N., Raymond, P. A., & Crowther, T. W. (2016). Managing uncertainty in soil carbon feedbacks to climate change. *Nature Climate Change*, 6(8), 751–758. https://doi.org/10.1038/nclimate3071

Brouwer, B., Ziolkowska, A., Bagard, M., Keech, O., & Gardeström, P. (2012). The impact of light intensity on shade-induced leaf senescence. *Plant, Cell & Environment*, 35(6), 1084–1098. https://doi.org/10.1111/j.1365-3040.2011.02474.x

Cao, G., Giambelluca, T. W., Stevens, D. E., & Schroeder, T. A. (2007). Inversion variability in the Hawaiian trade wind regime. *Journal of Climate*, 20(7), 1145–1160. https://doi.org/10.1175/JCLI4033.1

Caprez, R., Niklaus, P. A., & Körner, C. (2012). Forest soil respiration reflects plant productivity across a temperature gradient in the Alps. *Oecologia*, 170(4), 1143–1154. https://doi.org/10.1007/s00442-012-2371-3

Chu, C., Bartlett, M., Wang, Y., He, F., Weiner, J., Chave, J., & Sack, L. (2016). Does climate directly influence NPP globally? *Global Change Biology*, 22(1), 12–24. https://doi.org/10.1111/gcb.13079

Cordell, S., Goldstein, G., Meinzer, F., & Vitousek, P. M. (2001). Regulation of leaf life-span and nutrient-use efficiency of Metrosideros polymorpha trees at two extremes of a long chronosequence in Hawaii. *Oecologia*, 127, 198–206. https://doi.org/10.1007/s004420000588

Cox, P. M., Pearson, D., Booth, B. B., Friedlingstein, P., Huntingford, C., Jones, C. D., & Luke, C. M. (2013). Sensitivity of tropical carbon to climate change constrained by carbon dioxide variability. *Nature*, 494(7437), 341–344. https://doi.org/10.1038/nature11882

Drake, J. E., Furze, M. E., Tjoelker, M. G., Carrillo, Y., Barton, C. V. M., & Pendall, E. (2019). Climate warming and tree carbon use efficiency in a whole tree [13]CO_2 tracer study. *New Phytologist*, 222(3), 1313–1324. https://doi.org/10.1111/nph.15721

Drake, J. E., Tjoelker, M. G., Aspinwall, M. J., Reich, P. B., Pfautsch, S., & Barton, C. V. M. (2019). The partitioning of gross primary production for young Eucalyptus tereticornis trees under experimental warming and altered water availability. *New Phytologist*, 222(3), 1298–1312. https://doi.org/10.1111/nph.15629

Estiarte, M., Vicca, S., Peñuelas, J., Bahn, M., Beier, C., Emmett, B. A., & Kröel-Dulay, G. (2016). Few multiyear precipitation–reduction experiments find a shift in the productivity–precipitation relationship. *Global Change Biology*, 22(7), 2570–2581. https://doi.org/10.1111/gcb.13269

Fahey, T. J., Sherman, R. E., & Tanner, E. V. J. (2016). Tropical montane cloud forest: environmental drivers of vegetation structure and ecosystem function. *Journal of Tropical Ecology*, 32(5), 355–367. https://doi.org/10.1017/S0266467415000176

Fissore, C., Giardina, C. P., & Kolka, R. (2013). Reduced substrate supply limits the temperature response of soil organic carbon decomposition. *Soil Biology & Biochemistry*, 67, 306–311. https://doi.org/10.1016/j.soilbio.2013.09.007

Fyllas, N. M., Bentley, L. P., Shenkin, A., Asner, G. P., Atkin, O. K., Díaz, S., Enquist, B. J., Farfan-Rios, W., Gloor, E., Guerrieri, R., Huasco, W. H., Ishida, Y., Martin, R. E., Meir, P., Phillips, O., Salinas, N., Silman, M., Weerasinghe, L. K., Zaragoza-Castells, J., & Malhi, Y. (2017). Solar radiation and functional traits explain the decline of forest primary productivity along a tropical elevation gradient. *Ecology Letters*, 20, 730–740. https://doi.org/10.1111/ele.12771

Gherardi, L. A., & Sala, O. E. (2020). Global patterns and climatic controls of belowground net carbon fixation. *Proceedings of the National Academy of Sciences of the United States of America*, 117(33), 20038–20043. https://doi.org/10.1073/pnas.2006715117

Giambelluca, T. W., Chen, Q., Frazier, A. G., Price, J. P., Chen, Y.-L., Chu, P.-S., Eischeid, J. K., & Delparte, D. M. (2013). Online rainfall atlas of Hawaii. *Bulletin of the American Meteorological Society*, 94, 313–316.

Giambelluca, T. W., Shuai, X., Barnes, M. L., Alliss, R. J., Longman, R. J., Miura, T., Chen, Q., Frazier, A. G., Mudd, R. G., Cuo, L., & Businger, A. D. (2014). Evapotranspiration of Hawai'i. Final report submitted to the U.S. Army Corps of Engineers—Honolulu District, and the Commission on Water Resource Management, State of Hawai'i.

Giardina, C. P., Binkley, D., Ryan, M., Fownes, J., & Senock, R. (2004). Belowground carbon cycling in a humid tropical forest decreases with fertilization. *Oecologia*, 139(4), 545–550. https://doi.org/10.1007/s00442-004-1552-0

Giardina, C. P., Litton, C. M., Crow, S. E., & Asner, G. P. (2014). Warming-related increases in soil CO_2 efflux are explained by increased belowground carbon efflux. *Nature Climate Change*, 4(9), 822–827. https://doi.org/10.1038/NCLIMATE2322

Giardina, C., & Ryan, M. (2000). Evidence that decomposition rates of organic carbon in mineral soil do not vary with temperature. *Nature*, 404(6780), 858–861. https://doi.org/10.1038/35009076

Giardina, C. P., & Ryan, M. G. (2002). Total belowground carbon allocation in a fast-growing Eucalyptus plantation estimated using a carbon balance approach. *Ecosystems*, 5(5), 487–499. https://doi.org/10.1007/s10021-002-0130-8

Giardina, C. P., Ryan, M. G., Binkley, D., & Fownes, J. H. (2003). Primary production and carbon allocation in relation to nutrient supply in a tropical experimental forest. *Global Change Biology*, 9(10), 1438–1450. https://doi.org/10.1046/j.1365-2486.2003.00558.x

Girardin, C. A. J., Malhi, Y., Aragão, L. E. O. C., Mamani, M., Huaraca huasco, W., Durand, L., Feeley, K. J., Rapp, J., Silva-espejo, J. E., Silman, M., Salinas, N., & Whittaker, R. J. (2010). Net primary productivity allocation and cycling of carbon along a tropical forest elevational transect in the Peruvian Andes. *Global Change Biology*, 16(12), 3176–3192. https://doi.org/10.1111/j.1365-2486.2010.02235.x

Goldsmith, G. R., Matzke, N. J., & Dawson, T. E. (2013). The incidence and implications of clouds for cloud forest plant water relations. *Ecology Letters*, 16(3), 307–314. https://doi.org/10.1111/ele.12039

Hartmann, H., Bahn, M., Carbone, M., & Richardson, A. D. (2020). Plant carbon allocation in a changing world – Challenges and progress: Introduction to a Virtual Issue on carbon allocation. *New Phytologist*, 227(4), 981–988. https://doi.org/10.1111/nph.16757

Hobbie, S. E., & Chapin, F. S. III (1998). The response of tundra plant biomass, aboveground production, nitrogen, and CO_2 flux to experimental warming. *Ecology*, 79(5), 1526–1544. https://doi.org/10.2307/176774

Högberg, P., Nordgren, A., Buchmann, N., Taylor, A. F. S., Ekblad, A., Högberg, M. N., Nyberg, G., Ottosson-Löfvenius, M., & Read, D. J. (2001). Large-scale forest girdling shows that current photosynthesis drives soil respiration. *Nature*, 411(6839), 789–792. https://doi.org/10.1038/35081058

Iwashita, D., Litton, C. M., & Giardina, C. P. (2013). Coarse woody debris carbon pools across a 5.2°C mean annual temperature gradient in tropical montane wet forest. *Forest Ecology and Management*, 291, 336–343. https://doi.org/10.1016/j.foreco.2012.11.043

Jung, M., Reichstein, M., Margolis, H. A., Cescatti, A., Richardson, A. D., Arain, M. A., Arneth, A., Bernhofer, C., Bonal, D., Chen, J., Gianelle, D., Gobron, N., Kiely, G., Kutsch, W., Lasslop, G., Law, B. E., Lindroth, A., Merbold, L., Montagnani, L., … Williams, C. (2011). Global patterns of land-atmosphere fluxes of carbon dioxide, latent heat, and sensible heat derived from eddy covariance, satellite,

and meteorological observations. *Journal of Geophysical Research*, *116*(G00J07), https://doi.org/10.1029/2010JG001566

Jung, M., Reichstein, M., Schwalm, C. R., Huntingford, C., Sitch, S., Ahlström, A., Arneth, A., Camps-Valls, G., Ciais, P., Friedlingstein, P., Gans, F., Ichii, K., Jain, A. K., Kato, E., Papale, D., Poulter, B., Raduly, B., Rödenbeck, C., Tramontana, G., ... Zeng, N. (2017). Compensatory water effects link yearly global land CO_2 sink changes to temperature. *Nature*, *541*(7638), 516–520. https://doi.org/10.1038/nature20780

Kannenberg, S. A., Schwalm, C. R., & Anderegg, W. R. (2020). Ghosts of the past: how drought legacy effects shape forest functioning and carbon cycling. *Ecology Letters*, *23*(5), 891–901. https://doi.org/10.1111/ele.13485

Knapp, A. K., Avolio, M. L., Beier, C., Carroll, C. J. W., Collins, S. L., Dukes, J. S., Fraser, L. H., Griffin-Nolan, R. J., Hoover, D. L., Jentsch, A., Loik, M. E., Phillips, R. P., Post, A. K., Sala, O. E., Slette, I. J., Yahdjian, L., & Smith, M. D. (2017). Pushing precipitation to the extremes in distributed experiments: Recommendations for simulating wet and dry years. *Global Change Biology*, *23*(5), 1774–1782. https://doi.org/10.1111/gcb.13504

Li, W., Zhang, H., Huang, G., Liu, R., Wu, H., Zhao, C., & Mcdowell, N. G. (2020). Effects of nitrogen enrichment on tree carbon allocation: A global synthesis. *Global Ecology and Biogeography*, *29*(3), 573–589. https://doi.org/10.1111/geb.13042

Liptzin, D., & Silver, W. L. (2015). Spatial patterns in oxygen and redox sensitive biogeochemistry in tropical forest soils. *Ecosphere*, *6*(11), 1–14. https://doi.org/10.1890/ES14-00309.1

Litton, C. M., & Giardina, C. P. (2008). Belowground carbon flux and partitioning: Global patterns and response to temperature. *Functional Ecology*, *22*(6), 941–954. https://doi.org/10.1111/j.1365-2435.2008.01479.x

Litton, C. M., Giardina, C. P., Albano, J. K., Long, M. S., & Asner, G. P. (2011). The magnitude and variability of soil-surface CO_2 efflux increase with mean annual temperature in Hawaiian tropical montane wet forests. *Soil Biology & Biochemistry*, *43*, 2315–2323. https://doi.org/10.1016/j.soilbio.2011.08.004

Litton, C. M., Giardina, C. P., Freeman, K. R., Selmants, P. C., & Sparks, J. P. (2020). Impact of mean annual temperature on nutrient availability in a tropical montane wet forest. *Frontiers in Plant Science*, *11*(11), 784. https://doi.org/10.3389/fpls.2020.00784

Litton, C. M., Raich, J. W., & Ryan, M. G. (2007). Carbon allocation in forest ecosystems. *Global Change Biology*, *13*(10), 2089–2109. https://doi.org/10.1111/j.1365-2486.2007.01420.x

Liu, J., Bowman, K. W., Schimel, D. S., Parazoo, N. C., Jiang, Z., Lee, M., Bloom, A. A., Wunch, D., Frankenberg, C., Sun, Y., O'Dell, C. W., Gurney, K. R., Menemenlis, D., Gierach, M., Crisp, D., & Eldering, A. (2017). Contrasting carbon cycle responses of the tropical continents to the 2015–2016 El Niño. *Science*, *358*(6360), eaam5690. https://doi.org/10.1126/science.aam5690

Liu, L., Wang, X., Lajeunesse, M. J., Miao, G., Piao, S., Wan, S., Wu, Y., Wang, Z., Yang, S., Li, P., & Deng, M. (2016). A cross-biome synthesis of soil respiration and its determinants under simulated precipitation changes. *Global Change Biology*, *22*(4), 1394–1405. https://doi.org/10.1111/gcb.13156

Liu, X., Yang, Z., Lin, C., Giardina, C. P., Xiong, D., Lin, W., Chen, S., Xu, C., Chen, G., Xie, J., Li, Y., & Yang, Y. (2017). Will nitrogen deposition mitigate warming-increased soil respiration in a young subtropical plantation? *Agricultural and Forest Meteorology*, *246*, 78–85. https://doi.org/10.1016/j.agrformet.2017.06.010

Luo, Y., Sherry, R., Zhou, X., & Wan, S. (2009). Terrestrial carbon-cycle feedback to climate warming: Experimental evidence on plant regulation and impacts of biofuel feedstock harvest. *Global Change Biology*, *1*(1), 62–74. https://doi.org/10.1111/j.1757-1707.2008.01005.x

Luyssaert, S., Inglima, I., Jung, M., Richardson, A. D., Reichstein, M., Papale, D., & Janssens, I. A. (2007). CO_2 balance of boreal, temperate, and tropical forests derived from a global

database. *Global Change Biology*, *13*(12), 2509–2537. https://doi.org/10.1111/j.1365-2486.2007.01439.x

Ma, Z., Chen, H. Y. H., Li, Y., & Chang, S. X. (2020). Interactive effects of global change factors on terrestrial net primary productivity are treatment length and intensity dependent. *Journal of Ecology*, *108*(5), 2083–2094. https://doi.org/10.1111/1365-2745.13379

Maes, W. H., & Steppe, K. (2012). Estimating evapotranspiration and drought stress with ground-based thermal remote sensing in agriculture: A review. *Journal of Experimental Botany*, *63*(13), 4671–4712. https://doi.org/10.1093/jxb/ers165

Melillo, J. M., Lu, X., Kicklighter, D. W., Reilly, J. M., Cai, Y., & Sokolov, A. P. (2016). Protected areas' role in climate-change mitigation. *Ambio*, *45*(2), 133–145. https://doi.org/10.1007/s13280-015-0693-1

Melillo, J. M., Steudler, P. A., Aber, J. D., Newkirk, K., Lux, H., Bowles, F. P., & Morrisseau, S. (2002). Soil warming and carbon-cycle feedbacks to the climate system. *Science*, *298*(5601), 2173–2176. https://doi.org/10.1126/science.1074153

Mitchard, E. T. (2018). The tropical forest carbon cycle and climate change. *Nature*, *559*(7715), 527–534. https://doi.org/10.1038/s41586-018-0300-2

Musavi, T., Migliavacca, M., Reichstein, M., Kattge, J., Wirth, C., Black, T. A., Janssens, I., Knohl, A., Loustau, D., Roupsard, O., Varlagin, A., Rambal, S., Cescatti, A., Gianelle, D., Kondo, H., Tamrakar, R., & Mahecha, M. D. (2017). Stand age and species richness dampen interannual variation of ecosystem-level photosynthetic capacity. *Nature Ecology & Evolution*, *1*(2), 0048. https://doi.org/10.1038/s41559-016-0048

Myneni, R. B., Yang, W., Nemani, R. R., Huete, A. R., Dickinson, R. E., Knyazikhin, Y., Didan, K., Fu, R., Negron Juarez, R. I., Saatchi, S. S., Hashimoto, H., Ichii, K., Shabanov, N. V., Tan, B., Ratana, P., Privette, J. L., Morisette, J. T., Vermote, E. F., Roy, D. P., ... Salomonson, V. V. (2007). Large seasonal swings in leaf area of Amazon rainforests. *Proceedings of the National Academy of Sciences of the United States of America*, *104*(12), 4820–4823. https://doi.org/10.1073/pnas.0611338104

Nemani, R. R., Keeling, C. D., Hashimoto, H., Jolly, W. M., Piper, S. C., Tucker, C. J., & Running, S. W. (2003). Climate-driven increases in global terrestrial net primary production from 1982 to 1999. *Science*, *300*(5625), 1560–1563. https://doi.org/10.1126/science.1082750

Norby, R. J., & Luo, Y. (2004). Evaluating ecosystem responses to rising atmospheric CO_2 and global warming in a multi-factor world. *New Phytologist*, *162*(2), 281–293. https://doi.org/10.1111/j.1469-8137.2004.01047.x

Nottingham, A. T., Meir, P., Velasquez, E., & Turner, B. L. (2020). Soil carbon loss by experimental warming in a tropical forest. *Nature*, *584*(7820), 234–237. https://doi.org/10.1038/s41586-020-2566-4

Ogle, K. (2018). Hyperactive soil microbes might weaken the terrestrial carbon sink. *Nature*, *560*(7716), 32–33. https://doi.org/10.1038/d41586-018-05842-2

Oliphant, A., Dragoni, D., Deng, B., Grimmond, C., Schmid, H. P., & Scott, S. (2011). The role of sky conditions on gross primary production in a mixed deciduous forest. *Agricultural and Forest Meteorology*, *151*, 781–791. https://doi.org/10.1016/j.agrformet.2011.01.005

Piao, S., Wang, X., Wang, K., Li, X., Bastos, A., Canadell, J. G., Ciais, P., Friedlingstein, P., & Sitch, S. (2020). Interannual variation of terrestrial carbon cycle: Issues and perspectives. *Global Change Biology*, *26*(1), 300–318. https://doi.org/10.1111/gcb.14884

Pierre, S., Hewson, I., Sparks, J. P., Litton, C. M., Giardina, C., Groffman, P. M., & Fahey, T. J. (2017). Ammonia oxidizer populations vary with nitrogen cycling across a tropical montane mean annual temperature gradient. *Ecology*, *98*(7), 1896–1907. https://doi.org/10.1002/ecy.1863

Poulter, B., Frank, D., Ciais, P., Myneni, R. B., Andela, N., Bi, J., Broquet, G., Canadell, J. G., Chevallier, F., Liu, Y. Y., Running, S. W., Sitch,

S., & van der Werf, G. R. (2014). Contribution of semi-arid ecosystems to interannual variability of the global carbon cycle. *Nature*, *509*(7502), 600–603. https://doi.org/10.1038/nature13376

Raich, J. W., & Nadelhoffer, K. J. (1989). Belowground carbon allocation in forest ecosystems: global trends. *Ecology*, *70*, 1346–1354.

Raich, J. W., Russell, A. E., & Vitousek, P. M. (1997). Primary productivity and ecosystem development along an elevational gradient on Mauna Loa, Hawai'i. *Ecology*, *78*(3), 707–721. https://doi.org/10.1890/0012-9658(1997)078[0707:PPAEDA]2.0.CO;2

Reich, P. B., Hobbie, S. E., Lee, T. D., Rich, R., Pastore, M. A., & Worm, K. (2020). Synergistic effects of four climate change drivers on terrestrial carbon cycling. *Nature Geoscience*, *13*(12), 787–793. https://doi.org/10.1038/s41561-020-00657-1

Richardson, A. D., Hollinger, D. Y., Aber, J. D., Ollinger, S. V., & Braswell, B. H. (2007). Environmental variation is directly responsible for short- but not long-term variation in forest-atmosphere carbon exchange. *Global Change Biology*, *13*(4), 788–803. https://doi.org/10.1111/j.1365-2486.2007.01330.x

Rillig, M. C., Ryo, M., Lehmann, A., Aguilar-Trigueros, C. A., Buchert, S., Wulf, A., Iwasaki, A., Roy, J., & Yang, G. (2019). The role of multiple global change factors in driving soil functions and microbial biodiversity. *Science*, *366*(6467), 886–890. https://doi.org/10.1126/science.aay2832

Rustad, L., Campbell, J., Marion, G., Norby, R., Mitchell, M., Hartley, A., Cornelissen, J., & Gurevitch, J. (2001). A meta-analysis of the response of soil respiration, net nitrogen mineralization, and aboveground plant growth to experimental ecosystem warming. *Oecologia*, *126*(4), 543–562. https://doi.org/10.1007/s004420000544

Sala, O. E., Gherardi, L. A., Reichmann, L., Jobbagy, E., & Peters, D. (2012). Legacies of precipitation fluctuations on primary production: Theory and data synthesis. *Philosophical Transactions of the Royal Society B: Biological Sciences*, *367*(1606), 3135–3144. https://doi.org/10.1098/rstb.2011.0347

Schuur, E. (2001). The Effect of Water on Decomposition dynamics in mesic to wet Hawaiian montane forests. *Ecosystems*, *4*, 259–273. https://doi.org/10.1007/s10021-001-0008-1

Selmants, P. C., Adair, K. L., Litton, C. M., Giardina, C. P., & Schwartz, E. (2016). Increases in mean annual temperature do not alter soil bacterial community structure in tropical montane wet forests. *Ecosphere*, *7*(4), e01296. https://doi.org/10.1002/ecs2.1296

Selmants, P. C., Litton, C. M., Giardina, C. P., & Asner, G. P. (2014). Ecosystem carbon storage does not vary with mean annual temperature in Hawaiian tropical montane wet forests. *Global Change Biology*, *20*(9), 2927–2937. https://doi.org/10.1111/gcb.12636

Sistla, S. A., Moore, J. C., Simpson, R. T., Gough, L., Shaver, G. R., & Schimel, J. P. (2013). Long-term warming restructures Arctic tundra without changing net soil carbon storage. *Nature*, *497*(7451), 615–618. https://doi.org/10.1038/nature12129

Skelton, R. P., Brodribb, T. J., McAdam, S. A., & Mitchell, P. J. (2017). Gas exchange recovery following natural drought is rapid unless limited by loss of leaf hydraulic conductance: Evidence from an evergreen woodland. *New Phytologist*, *215*(4), 1399–1412. https://doi.org/10.1111/nph.14652

Sokol, N. W., & Bradford, M. A. (2019). Microbial formation of stable soil carbon is more efficient from belowground than aboveground input. *Nature Geoscience*, *12*(1), 46–53. https://doi.org/10.1038/s41561-018-0258-6

Song, J., Wan, S., Piao, S., Knapp, A. K., Classen, A. T., Vicca, S., Ciais, P., Hovenden, M. J., Leuzinger, S., Beier, C., Kardol, P., Xia, J., Liu, Q., Ru, J., Zhou, Z., Luo, Y., Guo, D., Adam Langley, J., Zscheischler, J., … Zheng, M. (2019). A meta-analysis of 1,119 manipulative experiments on terrestrial carbon-cycling responses to global change. *Nature Ecology & Evolution*, *3*, 1309–1320. https://doi.org/10.1038/s41559-019-0958-3

Sullivan, M. J. P., Lewis, S. L., Affum-Baffoe, K., Castilho, C., Costa, F., Sanchez, A. C., Ewango, C. E. N., Hubau, W., Marimon, B., Monteagudo-Mendoza, A., Qie, L., Sonké, B., Martinez, R. V., Baker, T. R., Brienen, R. J. W., Feldpausch, T. R., Galbraith, D., Gloor, M., Malhi, Y., … Phillips, O. L. (2020). Long-term thermal sensitivity of Earth's tropical forests. *Science*, *368*(6493), 869–874. https://doi.org/10.1126/science.aaw7578

Taylor, P. G., Cleveland, C. C., Wieder, W. R., Sullivan, B. W., Doughty, C. E., Dobrowski, S. Z., & Townsend, A. R. (2017). Temperature and rainfall interact to control carbon cycling in tropical forests. *Ecology Letters*, *20*(6), 779–788. https://doi.org/10.1111/ele.12765

Toszogyova, A., & Storch, D. (2019). Global diversity patterns are modulated by temporal fluctuations in primary productivity. *Global Ecology and Biogeography*, *28*(12), 1827–1838. https://doi.org/10.1111/geb.12997

Walker, T. W. N., Janssens, I. A., Weedon, J. T., Sigurdsson, B. D., Richter, A., Peñuelas, J., Leblans, N. I. W., Bahn, M., Bartrons, M., De Jonge, C., Fuchslueger, L., Gargallo-Garriga, A., Gunnarsdóttir, G. E., Marañón-Jiménez, S., Oddsdóttir, E. S., Ostonen, I., Poeplau, C., Prommer, J., Radujković, D., … Verbruggen, E. (2020). A systemic overreaction to years versus decades of warming in a subarctic grassland ecosystem. *Nature Ecology & Evolution*, *4*, 101–108. https://doi.org/10.1038/s41559-019-1055-3

Wang, J., Dong, J., Yi, Y., Lu, G., Oyler, J., Smith, W. K., Zhao, M., Liu, J., & Running, S. (2017). Decreasing net primary production due to drought and slight decreases in solar radiation in China from 2000 to 2012. *Journal of Geophysical Research: Biogeosciences*, *122*(1), 261–278. https://doi.org/10.1002/2016JG003417

Wolfe, E. W., & Morris, J. (1996). *Geologic map of the island of Hawaii*. US Geological Survey.

Wood, T. E., Cavaleri, M. A., Giardina, C. P., Khan, S., Mohan, J. E., Nottingham, A. T., & Slot, M. (2019). Soil warming effects on low-latitude forests with highly-weathered soils. In J. Mohan (Ed.), *Ecosystem consequences of soil warming: Microbes, vegetation, fauna and soil biogeochemistry* (pp. 385–439). Academic Press. https://doi.org/10.1016/B978-0-12-813493-1.00015-6

Wood, T. E., Cavaleri, M. A., & Reed, S. C. (2012). Tropical forest carbon balance in a warmer world: A critical review spanning microbial-to ecosystem-scale processes. *Biological Reviews*, *87*(4), 912–927. https://doi.org/10.1111/j.1469-185X.2012.00232.x

Yang, L., Lyu, M., Li, X., Xiong, X., Lin, W., Yang, Y., & Xie, J. (2020). Decline in the contribution of microbial residues to soil organic carbon along a subtropical elevation gradient. *Science of the Total Environment*, *749*, 141583. https://doi.org/10.1016/j.scitotenv.2020.141583

Ziegler, S. E., Benner, R., Billings, S. A., Edwards, K. A., Philben, M., Zhu, X., & Laganiere, J. (2017). Climate warming can accelerate carbon fluxes without changing soil carbon stocks. *Frontiers in Earth Science*, *5*, https://doi.org/10.3389/feart.2017.00002

SUPPORTING INFORMATION

Additional supporting information may be found online in the Supporting Information section.